

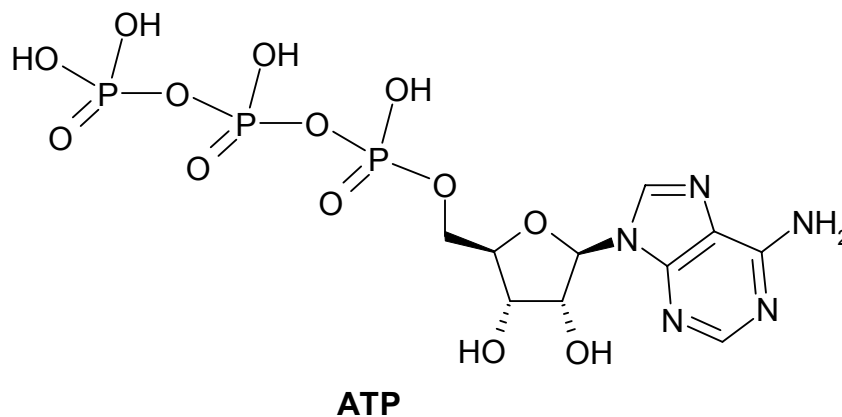
## Chapter 5

# Abiotic Synthesis of ATP from AMP in the Gas Phase: Implications for the Origin of Biologically Important Molecules from Small Molecular Clusters

Published previously in: Julian, R. R.; Beauchamp, J. L. *Int. J. Mass Spectrom.* **2003**, 227, 147-159.

### 5.1 Introduction

Adenosine 5'-triphosphate (ATP) is a ubiquitous biological molecule used for storing energy in the form of chemical bonds. The cellular machinery for creating ATP has been found in the oldest forms of life, yet it is still found in all groups of present day organisms.<sup>1</sup> Despite this ancient lineage and the extreme importance of ATP in many biological processes, it is surprising that the molecular mechanism for the synthesis of ATP is still open to debate.<sup>2,3</sup> Even more puzzling is how ATP originally became the primary energy currency for all of life.<sup>4</sup> In order to develop a more complete picture of the role of ATP in the origin of life, it is of interest to identify prebiotic routes that may have possibly contributed to the generation of ATP.



Several explanations for the terrestrial synthesis of thermodynamically unstable phosphoanhydride bonds have been given<sup>5,6</sup> and disputed.<sup>7</sup> The primary difficulty associated with the production of ATP on earth is that this type of chemistry is unlikely to occur in water. Not only is the hydrolysis of ATP exothermic,<sup>8</sup> but the oceans of the primitive world contained pyrite, which catalyses the hydrolysis of phosphoanhydride bonds.<sup>9</sup> Rigorously non-aqueous organic solvents may be used for the synthesis of phosphoanhydride bonds,<sup>10</sup> but the availability of such environments may have been limited in the early earth. Perhaps the best approach to phosphoanhydride synthesis involves chemistry in which no solvent is present, a suggestion which will be explained shortly.

Space is an environment which can easily accommodate conditions which are devoid of solvent. The presence of organic molecules in comets and meteorites and the possible role of these organics in the origin of life have drawn much attention over the years.<sup>11</sup> Related work has shown that it is possible to synthesize nucleotides such as adenosine 5'-monophosphate (AMP) by simply exposing the precursor molecules on a thin film to open space.<sup>12</sup> Interestingly, all of the components necessary to synthesize ATP have been detected in meteorites. A wide variety of sugars and their acid and alcohol counterparts

have been detected in the Murchison and Murray meteorites.<sup>13</sup> Phosphates and alkyl phosphonic acids in many forms have been detected in various meteorites.<sup>14,15</sup> Nucleobases and other nitrogen heterocycles, including adenine, have been detected in meteorites as well,<sup>16</sup> and they have been synthesized in experiments approximating the conditions in space.<sup>17</sup>

Terrestrial phenomena can also account for the extraction of key chemical components into a solvent free state. For example, it has been suggested that aerosol particles produced by sea spray may have formed cell like reactors in which geochemistry may have evolved into biochemistry.<sup>18</sup> Interestingly, organics from meteorites have been observed to transfer into these aerosol particles in high concentrations.<sup>19</sup> However, if the organic content of an aerosol particle is low and thus insufficient to form a protective monolayer, then as the particle travels to a region of low humidity the water will evaporate away. This could eventually lead to small, desolvated salt clusters. This process is fundamentally analogous to sonic spray ionization (SSI) experiments which can be monitored by mass spectrometry in a controlled environment.<sup>20,21</sup> It is interesting to note that SSI experiments lead to a great enhancement in the formation of clusters when compared to other ionization methods.<sup>22</sup>

The gas phase study of non-covalently bound clusters is a rapidly expanding area in the field of mass spectrometry.<sup>23,24,25</sup> The chemistry of small, noncovalently bound clusters and the role that they may have played in the prebiotic origin of biopolymers is the subject of the present work. It is demonstrated that trimers of AMP will yield ATP exclusively under the appropriate conditions. Collision activated dissociation (CAD) is utilized to initiate the reactions.<sup>26</sup> Furthermore, this chemistry is general in nature and can

be applied to the generation of other polyphosphates which are also of biological significance. It is postulated that other linear polymers of biological importance could be generated from small clusters in a similar manner.

## 5.2 Experimental Methodology

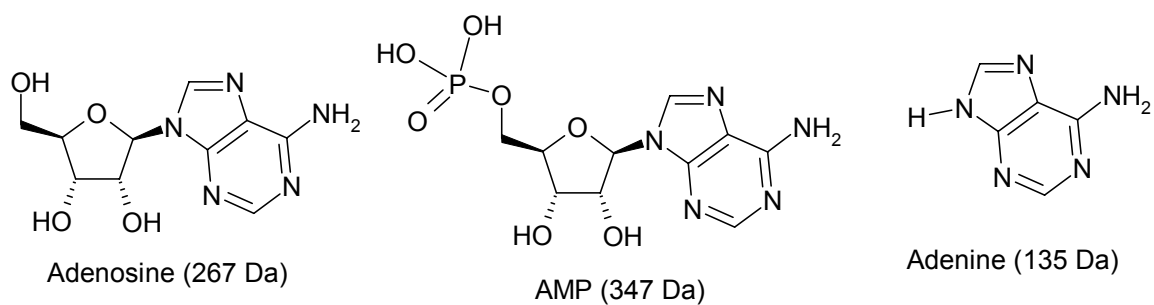
Mass spectra were obtained using a Finnigan LCQ ion trap quadrupole mass spectrometer without modification. The signal was optimized using the automatic tuning capabilities of the LCQ. To enhance cluster formation, the following settings were used for cationic clusters: source voltage 4.15 kV, capillary voltage 5.0 V, capillary temperature 200 °C, and tube lens offset -40 V. Collision activated dissociation was performed on isolated ions by applying a resonance excitation RF voltage of between 0.98 V and 2.45 V for a period of 30 ms.

Sample concentrations were in the range of ~50  $\mu$ M. Samples were electrosprayed using a 80:20 methanol/water mixture at a flow rate of 3  $\mu$ L/min from a 250  $\mu$ L Hamilton syringe. Silica tubing with an inner diameter of 12.7 microns inside a stainless steel sheath was used for electrospraying the mixture. Compounds were purchased commercially and used without further purification.

## 5.3 Results

**Anionic Clusters.** The negative ion ESI-MS spectrum for the sodium salt of AMP is shown in Figure 5.1a. The two major peaks correspond to  $[\text{AMP-H}]^-$  and  $[\text{2AMP-H}]^-$ . Clusters incorporating one or more sodium ions replacing protons are present in smaller abundance. Isolation of  $[\text{3AMP-H}]^-$  followed by CAD leads exclusively to the loss of

neutral AMP, as shown in Figure 5.1b. The results differ marginally when one hydrogen is replaced by sodium. The CAD spectrum for  $[3\text{AMP}-2\text{H}+\text{Na}]^-$  is shown in Figure 5.1c. The primary product is the loss of neutral AMP. However, there is also a minor loss of 267 Da, which corresponds to the loss of an adenosine nucleoside. In other words, one AMP has been fragmented, releasing neutral adenosine and leaving  $\text{PO}_3$  with the cluster. The structures for AMP and two important fragments are given below.



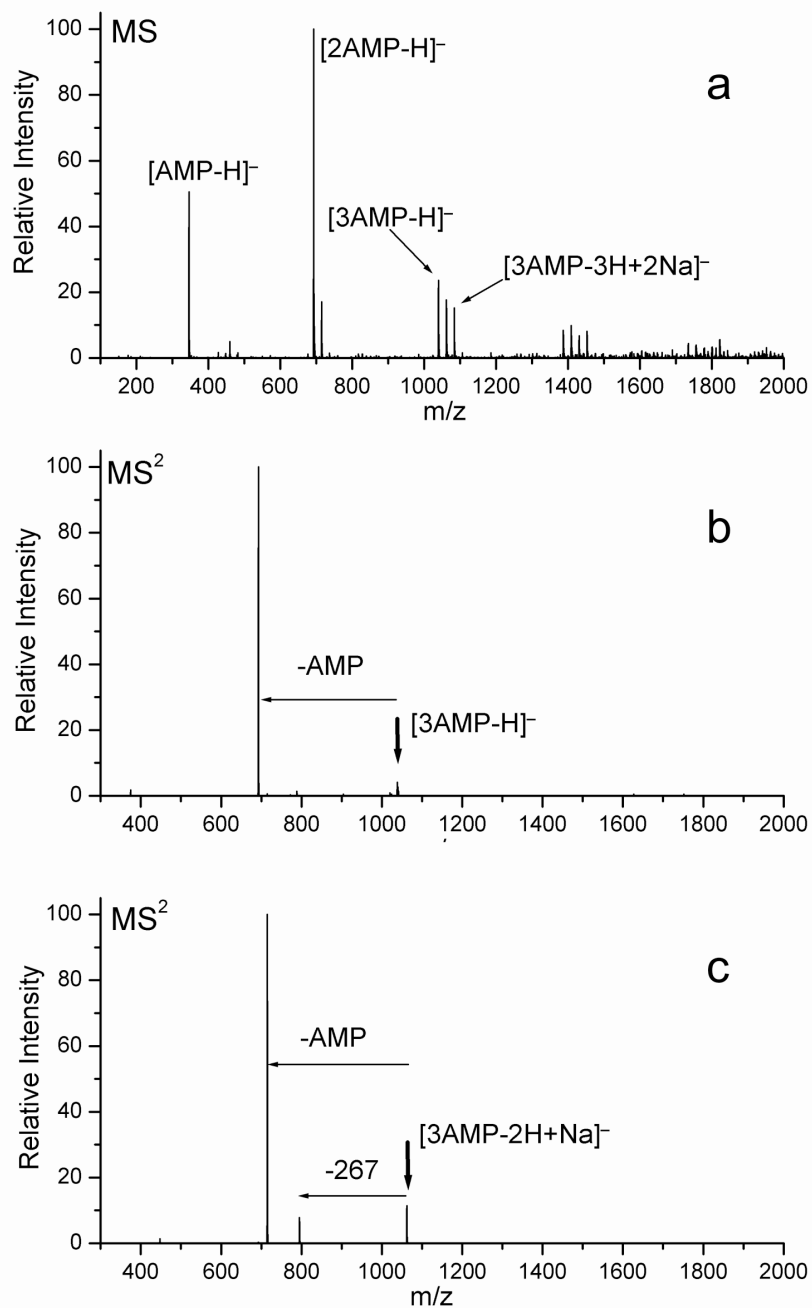


**Figure 5.1** (a) Anionic clusters of AMP with sodium. (b) CAD spectrum of the deprotonated AMP trimer showing that no covalent bonds are broken. (c) CAD spectrum of AMP trimer with inclusion of one sodium ion, in which a minor peak corresponding to the fragmentation of one AMP (namely, loss of adenosine) is observed.

Figure 5.2 shows the results for the sequential CAD of the  $[3\text{AMP}-3\text{H}+2\text{Na}]^-$ . The loss of adenosine leads to the base peak in Figure 5.2a. Some additional loss of a second adenosine is observed in Figure 5.2a as well. The primary product is isolated in Figure 5.2b. Further CAD in Figure 5.2c leads exclusively to the loss of the second adenosine. Tentatively, the results in these spectra correspond to the transformation of 3AMP into AMP+ADP, which is then converted into ATP, as will be discussed in greater detail below.

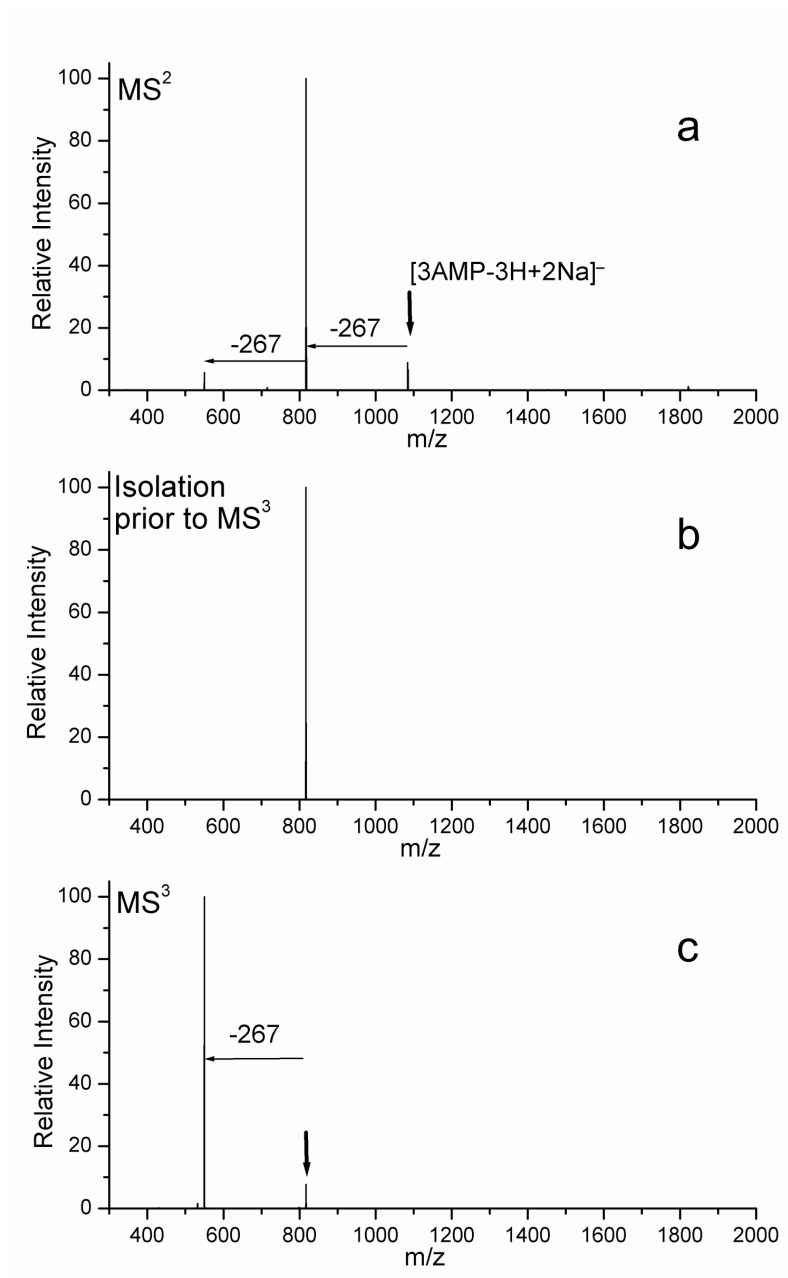


**Figure 5.2** (a) CAD spectrum of the anionic sodiated salt cluster of the AMP trimer. The loss of adenosine is predominant and no dissociation of the cluster by loss of AMP is observed. (b) Isolation of the product peak. (c) MS<sup>3</sup> spectrum demonstrating the loss of a second adenosine and the generation of ATP.



Three additional collisional activation steps are performed on the primary product from Figure 5.2c in Figure 5.3. The primary peak in Figure 5.3a results from the loss of 18 Da (water). An additional loss of 102 Da is also observed. In Figure 5.3b, the adenine base is lost, leading to the base peak in the spectrum. This loss is accompanied by the pickup of water and methanol, yielding peaks with masses that are 18 Da and 32 Da higher than the daughter fragment, respectively.<sup>27</sup> Isolation of the daughter fragment does not eliminate these peaks, confirming that they are picked up from residual solvent in the trap. A competitive loss of 102 Da is also observed. Isolation of the most abundant product, followed by collisional activation yields primarily a loss 102 Da in the MS<sup>6</sup> spectrum shown in Figure 5.3c. An additional minor peak corresponding to the loss of a second 102 Da is also present in Figure 5.3c. This 102 Da most likely corresponds to neutral loss of NaPO<sub>3</sub>.

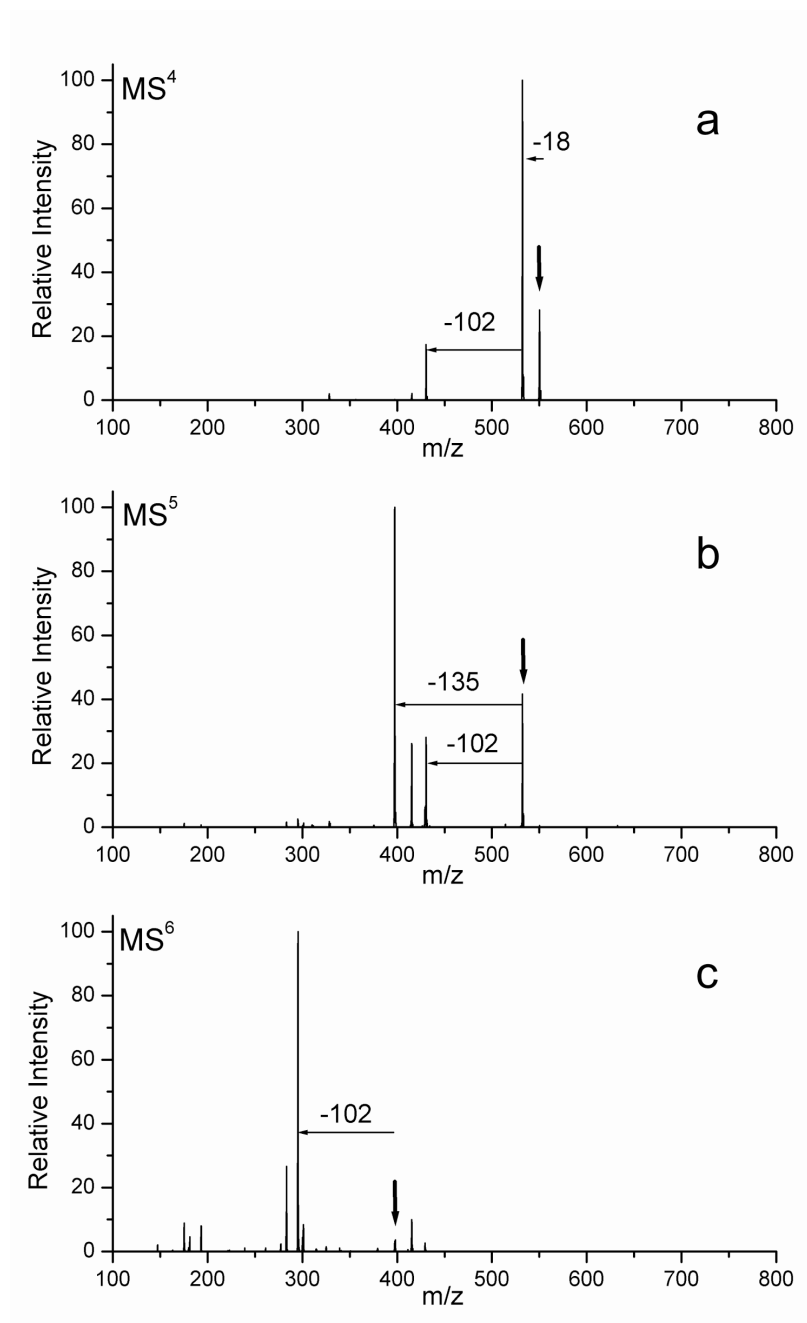


**Figure 5.3** Three further collisional activation steps on the product (ATP) generated in Figure 5.2c. (a) The lowest energy pathway leads to the loss of water. (b) Adenine is lost next. (c) Sequential losses of 102 Da or NaPO<sub>3</sub> are the final losses that are observed in this MS<sup>6</sup> spectrum.

The sequential CAD of an authentic sample of ATP is shown in Figure 5.4. In Figure 5.4a, isolation of  $[\text{ATP-3H+2Na}]^-$  is accompanied by the isobaric doubly charged dimer  $[\text{2ATP-6H+4Na}]^{2-}$ . Therefore, several of the daughter peaks in the CAD spectrum in Figure 4a result from the dissociation of the doubly charged dimer and are marked with a double asterisk. The loss of water leads to the base peak, just as in Figure 5.3a. In Figure 5.4b, interference from doubly charged peaks has been eliminated, and the spectrum is nearly identical to that shown in Figure 5.3b. Similarly, Figure 5.4c is very comparable to Figure 5.3c. In fact, even the majority of the minor peaks in both Figures 5.4b and 5.4c are identical to those found in Figures 5.3b and 5.3c.

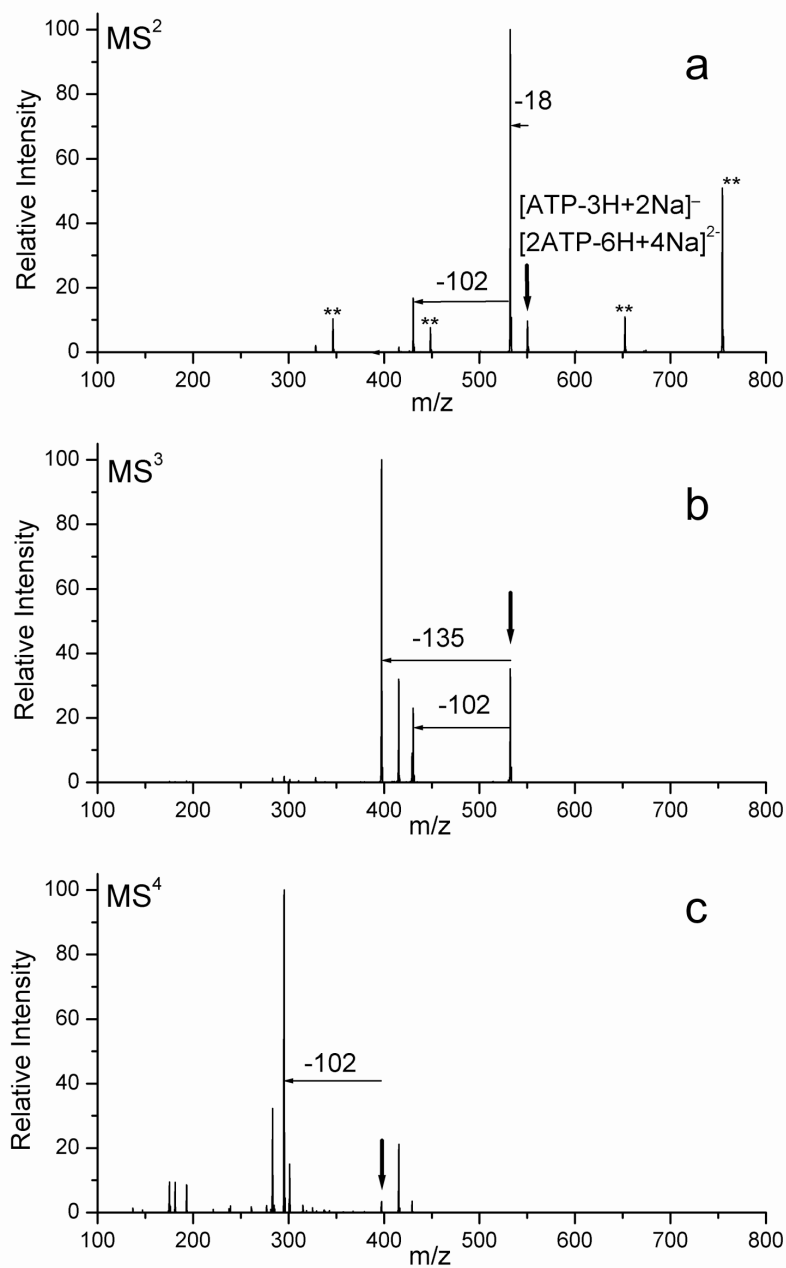


**Figure 5.4** Three CAD steps on authentic ATP,  $[\text{ATP-3H+2Na}]^-$ . (a) Some interference from the doubly charged dimer leads to additional peaks. (b) The loss of adenine is very abundant, as is also observed in Figure 5.3b. (c) Loss of 102 Da is observed in a similar fashion as Figure 5.3c, suggesting that the product produced in Figure 5.2c is in fact ATP. \*\* Daughter ions from the doubly charged dimer are indicated by a double asterisk.

**Cationic Clusters.** Figure 5.5 shows the positive ion ESI spectrum for the sodium salt of AMP. Clusters with a sodium cation providing the net charge are easily generated. Clusters incorporating up to five AMP molecules are observed. The maximum intensity for each cluster distribution corresponds to the peak fitting  $[x\text{AMP}-x\text{H}+(x+1)\text{Na}]^+$ , where  $x = 1-5$ . Formally then, each AMP is deprotonated and coupled with a sodium cation, forming salt clusters.

In Figure 5.5b, results are presented for the collisional activation of the cluster  $[3\text{AMP}-3\text{H}+4\text{Na}]^+$ . The loss of adenosine yields the most abundant product. Isolation of this product, followed by further collisional activation, leads primarily to the loss of another adenosine as seen in Figure 5.5c. These losses are identical to those observed in Figure 5.2 for the anionic clusters. The base peak produced in Figure 5.5c is isobaric with  $[\text{ATP}-3\text{H}+4\text{Na}]^+$ . Further CAD of this peak yields products that are indistinguishable from those produced by CAD of  $[\text{ATP}-3\text{H}+4\text{Na}]^+$  using an authentic ATP sample. The results for the cationic clusters closely parallel those obtained for the anionic clusters.

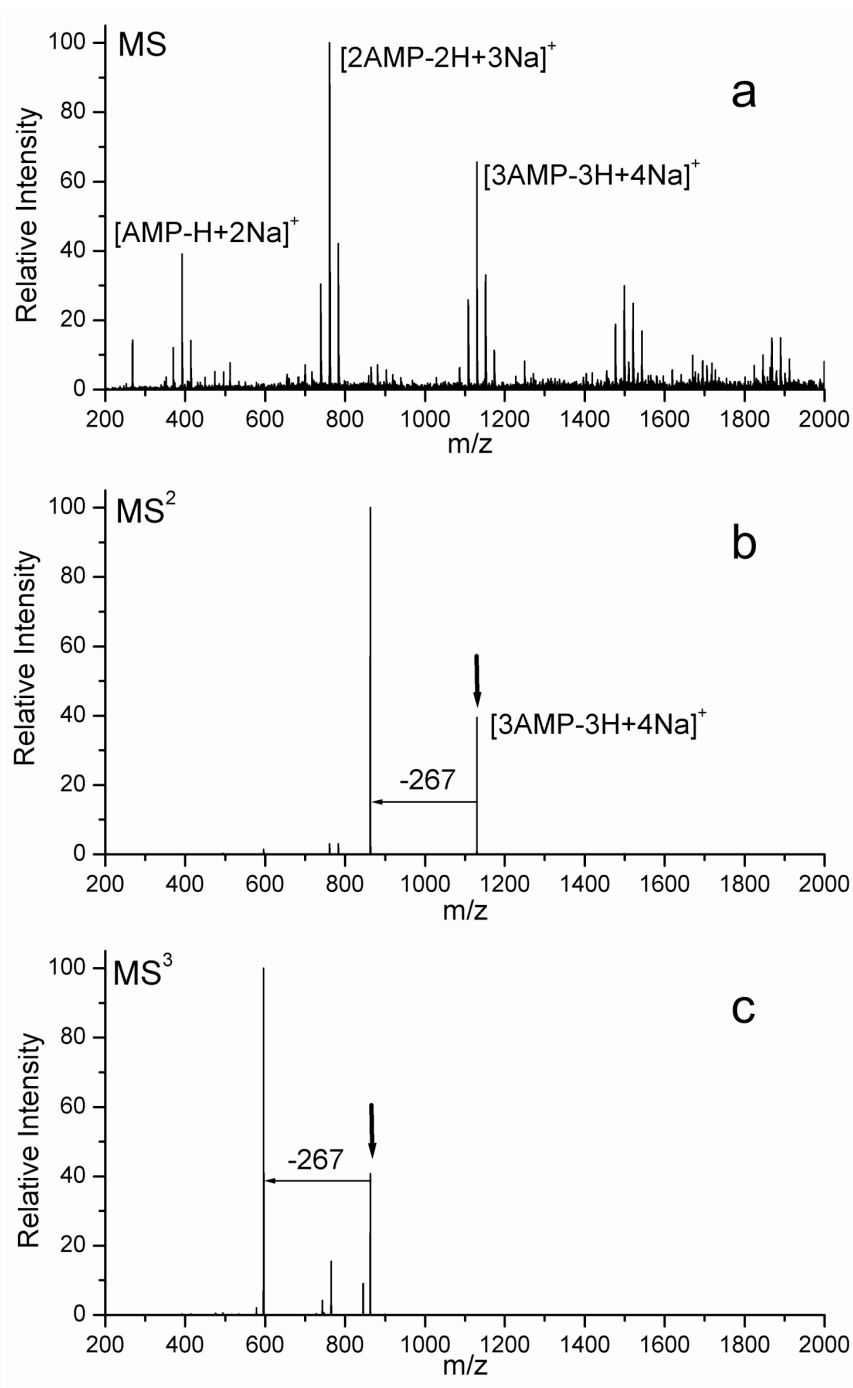


**Figure 5.5** (a) Sodiated cationic salt clusters of AMP. (b) CAD of the trimer leads to the formation of ADP+AMP. (c) A second adenosine is lost, implying that ATP is generated in high yield by a reaction similar to that observed for the anions.

**Phosphate Clusters.** The CAD spectra for clusters of phosphate are shown in Figure 5.6. The sodiated cluster  $[3\text{H}_2\text{PO}_4+\text{Na}]^-$  loses water exclusively as shown in Figure 5.6a. Subsequent activation of the daughter ion results in the loss of another water and the formation of triphosphate as shown in Figure 5.6b. This loss is accompanied by the pick up of water and methanol in low abundance. It is unclear whether the added solvent molecules react with the cluster or are merely coordinated to it. In Figure 5.6c,  $[3\text{H}_3\text{PO}_4-\text{H}]^-$  is subjected to CAD. In the absence of the sodium ions, the only observed product corresponds to a loss of  $\text{H}_3\text{PO}_4$ . These results closely parallel those observed for the AMP clusters.

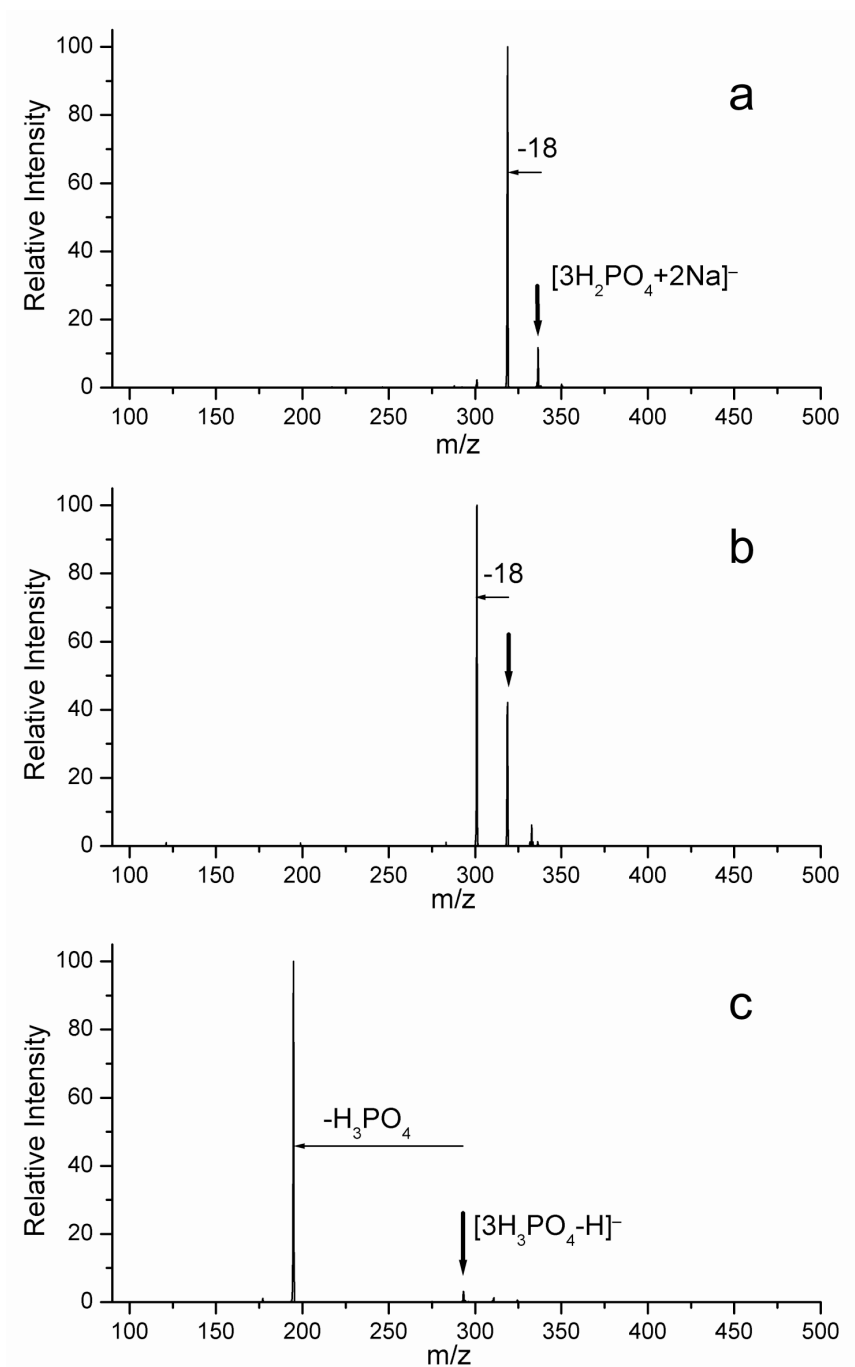


**Figure 5.6** (a) CAD spectrum of  $[3\text{H}_2\text{PO}_4 + \text{Na}]^-$  which loses water to form a phosphoanhydride. (b) CAD of the daughter ion from (a), yielding triphosphate from the loss of second water. (c) CAD of  $[3\text{H}_3\text{PO}_4 - \text{H}]^-$ . The hydrogen bound cluster simply dissociates by the loss of  $\text{H}_3\text{PO}_4$ .



**Calculations.** The enthalpic contributions to reaction 5.1 were calculated at the PM5 semi-empirical level and utilizing density functional theory at the BLYP/DZVP and B3LYP/6-31G\*\* levels. The results are given in Table 5.1. Methylphosphate is used instead of AMP to evaluate the binding energies of the clusters in order to allow for higher levels of theory to be utilized in a reasonable time. This approximation is supported by the experimental results shown in Figure 5.6 which suggest that most of the chemistry takes place in the phosphate/sodium salt portion of the clusters. The calculations reveal that metal bound phosphate salt clusters are more strongly bound in the gas phase than the proton bound counterparts. The PM5 methodology is sufficient to qualitatively predict the results, although the energetic ordering among the alkali metals is not correct.

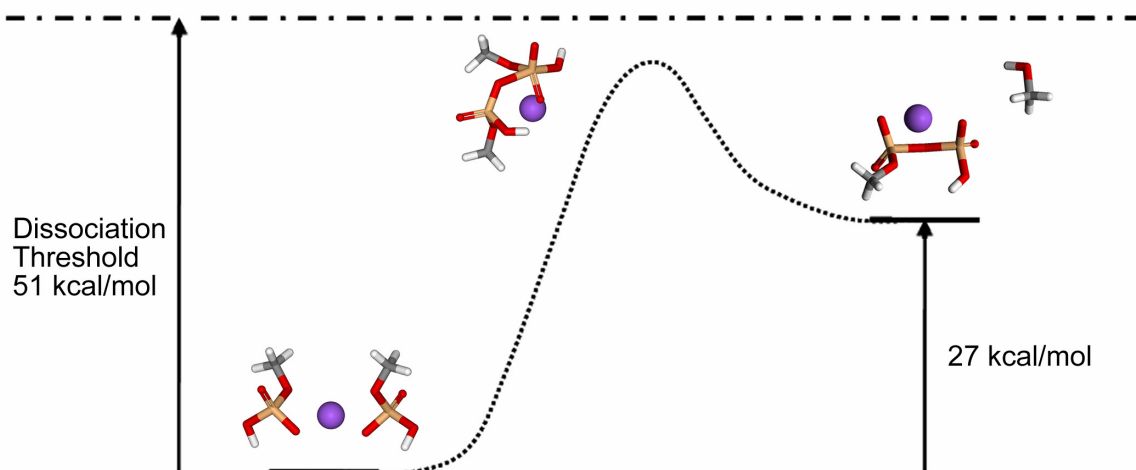


**Table 5.1 Calculated Energetics in kcal/mol**

Cluster	Binding Energy PM5	Binding Energy BLYP/DZVP	Binding Energy B3LYP/6-31G**
$(CH_3OPO_3H)_2H^-$	-22.36	-34.2309	-40.2867
$(CH_3OPO_3H)_2Li^-$	-46.37	-48.1216	-54.807
$(CH_3OPO_3H)_2Na^-$	-44.95	-44.9093	-50.7288
$(CH_3OPO_3H)_2K^-$	-46.71	-46.0386	-46.6662 <sup>a</sup>
$(CH_3OPO_3H)_2Rb^-$	-59.17	-41.0822	-38.2897 <sup>a</sup>

<sup>a</sup> Calculated using the LACVP basis set

The calculated energetics and structures for the collision induced reaction of  $[2CH_3HPO_4+Na]^-$  to yield  $[CH_3HPO_3PO_4+Na]^-$  and methanol are given in Scheme 5.1 in kcal/mol utilizing DFT at the B3LYP/6-31G\*\* level. The reaction is uphill, and proceeds via a metastable penta-coordinate phosphorous intermediate.

**Scheme 5.1** Reaction Coordinate Diagram for Model Chemical System\*

\*Calculated at the B3LYP/6-31G\*\* level,  $\Delta H$  given in kcal/mol

#### 5.4 Discussion.

The binding energy of a noncovalent cluster must be greater than the activation barrier for a reaction to occur by collisional activation. In CAD experiments with clusters, rearrangement processes involving the cleavage of covalent bonds are usually not competitive with dissociation of the complex.<sup>28</sup> This is well illustrated in Figure 5.1, where the hydrogen bonded clusters are shown to simply dissociate into the constituent molecules. The addition of a single sodium ion increases the binding energy sufficiently to allow some covalent bond cleavage, as seen in Figure 5.1c. However, the formation of a true salt cluster in Figure 5.2 lends greater binding energy to the cluster, enabling reactions with higher activation barriers. The greater binding energy is quantified by the computational results, which predict the salt cluster to be more strongly bound than the hydrogen bound cluster by roughly  $\sim 10$  kcal/mol for each substitution. As a result, in Figure 5.2 the sequential loss of two adenosine nucleosides which results from the

fragmentation of covalent bonds is observed almost exclusively. The final peak produced in Figure 5.2c appears to be ATP, but the fact that it has the same mass is not necessarily proof of structure.

In order to address that question, further CAD experiments and calculations were performed. The results for the calculations are shown in Scheme 5.1 as a reaction coordinate diagram. Theory predicts that the  $\Delta H$  for the reaction of a sodium bound dimer is significantly uphill, which is to be expected. The exact energy for the transition state was not calculated, but the transition state must lie below the dissociation threshold for the cluster and probably involves a penta-coordinate phosphorous as shown in Scheme 5.1.

The quasimolecular ion produced in Figure 5.2c and actual ATP were both subjected to further steps of CAD for comparison. The results from these experiments are presented in Figure 5.3 and Figure 5.4. With the exception of the peaks originating from the doubly charged cluster of ATP in Figure 5.4a, the spectra in both Figures are nearly identical. The peaks that are produced and the relative intensity of those peaks are very similar, including peaks that only constitute minor contributions to the total ion intensity. Although this is not absolute proof that the structure of the product in Figure 5.2c is ATP, it provides strong support for the conjecture.

Further support for this notion is obtained from the cationic clusters. Despite a different number of sodium ions and presence of net positive charge, the same chemistry is observed in sodiated clusters of AMP. Figure 5.5 clearly shows a favorable route to what appears to be ATP. Again, comparison of the subsequent CAD of this molecule with a verified sample of ATP reveals that the two yield identical daughter ions. There is

no interference from a dimer in this case, and the peaks and relative intensities of the daughter ions are nearly identical. This strongly suggests that ATP is indeed formed from the salt cluster trimer. The notion that two different products would coincidentally produce spectra that overlap exactly with ATP is unlikely.

Other important observations are related to the fact that the same chemistry operates in cationic and anionic clusters. This suggests that the net charge does not play a significant role in the mechanism that leads to the generation of ATP. Neutral clusters would probably yield similar results, but unfortunately neutral clusters are not well suited for the experiments performed in the present work. This does not preclude the formation of such clusters in the atmosphere, either from meteorites or sea spray, or the subsequent chemistry that follows. The results obtained in the present work suggest a viable prebiotic route to the synthesis of ATP.

Furthermore, the chemistry is not limited to the formation of ATP. In fact, it was possible to synthesize adenosine pentaphosphate, although the structure of this compound was not verified for lack of a sample for comparison. Other nucleotides and deoxynucleotides were basically interchangeable with AMP, allowing for the synthesis of other polyphosphates. Sodiated clusters of 5'-ribose-phosphate also yielded ribose polyphosphate upon collisional activation. Polyphosphate, another important and ubiquitous biopolymer,<sup>5</sup> can be synthesized from sodium salt clusters of phosphate itself. The facile generation of polyphosphates by this mechanism is therefore applicable to a wide range of biologically relevant molecules.

## 5.5 Conclusion.

ATP is easily generated by collisional activation of a sodiated salt cluster containing three AMP precursors. The sequential loss of two adenosines leads to the formation of ATP. Comparison of several subsequent steps of CAD dissociation of ATP generated by this method with that of actual ATP reveals that the two ions produce identical CAD spectra. This is true for ATP generated from both cationic and anionic sodiated salt clusters of AMP. Polyphosphates can also be generated by collisional activation of sodiated clusters of phosphate, ribose phosphate, and other nucleotides and deoxynucleotides.

This type of chemistry represents a feasible pathway for the generation of biologically important polymers. A potential prebiotic source for ATP or other polyphosphates is outlined in the present work, but conceivably other biopolymers may be generated by similar reactions. It is interesting to note that small clusters of biomolecules can have an inherent preference for homochirality, as is demonstrated by the serine octamer.<sup>29</sup> It appears quite possible that the chemistry of these small clusters may be more important than has been previously realized.

## 5.6 References

- 
- <sup>1</sup> Gogarten, J. P.; Taiz, L. *Photosynthesis Research* **1992**, *33*, 137-146.
- <sup>2</sup> Senior, A. L.; Nadanaciva, S.; Weber, J. *Biochim. Biophys. Acta* **2002**, *1553*, 188-211.
- <sup>3</sup> J. E. Walker (Ed.), *Biochim. Biophys. Acta* **2000**, *1458(2-3)*, entire special issue.
- <sup>4</sup> Muller, A. W. J. *Prog. Biophys. Molec. Biol.* **1995**, *63*, 193-231.
- <sup>5</sup> Kornberg, A.; Rao, N. N.; Ault-Riche, D. *Annu. Rev. Biochem.* **1999**, *68*, 89-125.
- <sup>6</sup> Yamagata, Y.; Watando, H.; Saitoh, M.; Namba, T. *Nature*, **1991**, *352*, 516-519.
- <sup>7</sup> Keefe, A. D.; Miller, S. L. *J. Mol. Evol.* **1995**, *41*, 693-702.
- <sup>8</sup> St Martin, H.; Ortega-Blake, I.; Les, A.; Adamowicz, L. *Biochim. Biophys. Acta* **1994**, *1207*, 12-23.
- <sup>9</sup> Tassis, A. C.; Penteado-Fava, A.; Pontes-Buarque, M.; Amorim, H. S. De; Bonapace, J. A. P.; Souza-Barros, F. De; Vieyra, A. *Origins Life Evol. B.* **1999**, *29*, 361-374.
- <sup>10</sup> Machado, V. G. M.; Bunton, C. A.; Zucco, C.; Nome, F. *J. Chem. Soc., Perk. Trans. 2*, **2000**, 169-173.
- <sup>11</sup> (a) Oro, J. *Nature*, **1961**, *190*, 389-390. (b) Delsemme, A. H. *Orgins Life* **1984**, *14*, 51-60. (c) Kissel, J.; Krueger, F. R. *Nature*, **1987**, *326*, 753-760. (d) Engel, M. H.; Macko, S. A. *Nature*, **1997**, *389*, 265-268. (e) Chyba, C. F.; Sagan, C. *Nature*, **1992**, *355*, 125-132.
- <sup>12</sup> Kuzicheva, E. A.; Simakov, M. B. *Adv. Space Res.* **1999**, *23*, 387-391.
- <sup>13</sup> Cooper, G.; Kimmich, N.; Belisle, W.; Sarinana, J.; Brabham, K.; Garrel, L.; *Nature* **2001**, *414*, 879-883.
- <sup>14</sup> Mautner, M. N.; Sinaj, S. *Geochim. Cosmochim. Acta* **2002**, *66*, 3161-3174.
- <sup>15</sup> Cooper, G. W.; Onwo, W. M.; Cronin, J. R. *Geochim. Cosmochim. Acta* **1992**, *56*, 4109-4115.

- 
- <sup>16</sup> Sephton, M. A. *Nat. Prod. Rep.* **2002**, *19*, 292-311.
- <sup>17</sup> Levy, M.; Miller, S. L.; Oro, J. *J. Mol. Evol.* **1999**, *49*, 165-168.
- <sup>18</sup> (a) Ellison, G. B.; Tuck, A. F.; Vaida, V. , *J. Geophys. Res.* **1999**, *104*, 11633-11642.  
(b) Tuck, A. *Surv. Geophys.* **2002**, *23*, 379-409. (c) Gill, P.S.; Graedel, T.E.; Weschler, C.G. *Rev. Geophys.* **1983**, *21*, 903-920.
- <sup>19</sup> Murphy, D.M.: 2001, Extraterrestrial material and stratospheric aerosols, In: B. Peucker-Ehrenbrink (ed.), *Accretion of Extraterrestrial Matter Throughout Earth's History*: New York, Kluwer Academic, 2001.
- <sup>20</sup> Hirabayashi, A.; Sakairi, M.; Koizumi, H. *Anal. Chem.* **1995**, *67*, 2878-2882.
- <sup>21</sup> Shiea, J.; Chang, D. -Y.; Lin, C. -H.; Jiang, S. -J. *Anal. Chem.* **2001**, *73*, 4983-4987.
- <sup>22</sup> Takats, Z.; Nanita, S. C.; Cooks, R. G.; Schlosser, G.; Vekey, K. *Anal. Chem.* **2003**, *75*, 1514-1523.
- <sup>23</sup> (a) Schalley, C. A. *Mass Spectrom. Rev.* **2001**, *20*, 253-309. (b) Loo, J. A. *Int. J. Mass Spectrom.* **2000**, *200*, 175-186.
- <sup>24</sup> Loo, J. A. *Mass Spectrom. Rev.* **1997**, *16*, 1-23.
- <sup>25</sup> Vekey, K.; Czira, G. *Anal. Chem.* **1997**, *69*, 1700-1705.
- <sup>26</sup> (a) Kuntz, A. F.; Boynton, A. W.; David, G. A.; Colyer, K. E.; Poutsma, J. C. *J. Am. Soc. Mass Spectrom.* **2002**, *13*, 72-81. (b) Armentrout, P. B. *J. Am. Soc. Mass Spectrom.* **2000**, *11*, 371-379. (c) Vékey, K.; Czira, G. *Anal. Chem.* **1997**, *69*, 1700-1705. (d) Tao, W. A.; Zhang, D.; Wang, F.; Thomas, P. D.; Cooks, R. G. *Anal. Chem.* **1999**, *71*, 4427-4429. (e) Vitale, G.; Valina, A. B.; Huang, H.; Amunugama, R.; Rodgers, M. T. *J. Phys. Chem. A* **2001**, *105*, 11351-11364.
- <sup>27</sup> This phenomenon is often observed in ion traps, particularly with transition metal ions.

---

<sup>28</sup> (a) Wan, K. X.; Gross, M. L.; Shibue, T. *J. Am. Soc. Mass Spectrom.* **2000**, *11*, 450-457. (b) Gabelica, V.; De Pauw, E. *J. Am. Soc. Mass Spectrom.* **2002**, *13*, 91-98. (c) Penn, S. G.; He, F.; Green, M. K.; Lebrilla, C. B. *J. Am. Soc. Mass Spectrom.* **1997**, *8*, 244-252. (d) Julian, R. R.; May, J. A.; Stoltz, B. M.; Beauchamp, J. L. *Angew. Chem. Int. Ed.* **2003**, *42(9)*, 1012-1015.

<sup>29</sup> (a) Julian, R. R.; Hodyss, R.; Kinnear, B.; Jarrold, M. F.; Beauchamp, J. L. *J. Phys. Chem. B.* **2002**, *106*, 1219-1228. (b) Counterman, A. E.; Clemmer, D. E. *J. Phys. Chem. B.* **2001**, *105*, 8092-8096. (c) Schalley, C. A.; Weis, P. *Int. J. Mass. Spectrom.* **2002**, *221*, 9-19. (d) Cooks, R. G.; Zhang, D.; Kock, K. J.; Gozzo, F. C.; Eberlin, M. N. *Anal. Chem.* **2001**, *73*, 3646-3655.